

# Polyurethane Cationomers with Pendant Trimethylammonium Groups. 1. Fourier Transform Infrared Temperature Studies

R. J. Goddard and S. L. Cooper\*,†

Department of Chemical Engineering, University of Wisconsin–Madison,  
Madison, Wisconsin 53706

Received August 30, 1994; Revised Manuscript Received December 12, 1994<sup>®</sup>

**ABSTRACT:** Specific interactions are investigated in a series of polyether–polyurethane cationomers containing pendant trimethylammonium groups, with ion contents ranging from 0 to 0.88 mequiv/g, using Fourier transform infrared temperature studies. Hydrogen bonding of urethane N–H groups to urethane carbonyls, which has been extensively reported in conventional polyurethanes, is also evident in these materials. Additionally, the N–H stretching region shows significant contributions from N–H groups hydrogen bonded to ether oxygens of the soft segments in the homogeneous un-ionized polyurethane and to neutralizing anions in the cationomers. Spectral deconvolution and mass balances are used to obtain semiquantitative information on the extent of hydrogen bonding to the various proton acceptors as a function of temperature. As the temperature of the un-ionized sample is increased from 30 to 140 °C, hydrogen bonding of N–H groups to polyether oxygens decreases, while hydrogen bonding to urethane carbonyls increases. A similar redistribution of N–H hydrogen bonds, from the anion to carbonyl groups with increasing temperature, is observed for the cationomers. The results for each polymer are related to its chemical structure, thermomechanical properties, and morphology.

## Introduction

Polyurethane (PU) elastomers are linear multiblock copolymers of the type (AB)<sub>n</sub> where at the service temperature one block of the material is glassy or semicrystalline and the other block is soft or rubbery. Unfavorable interactions between the soft segments and hard segments lead to a microphase-separated structure where the hard domains act as physical crosslinks. Typical driving forces for microphase separation include a difference in the polarity of the two components, hydrogen bonding of urethane linkages, and crystallization of one or both of the segments. Ionic groups have also been incorporated in the hard segments of polyurethanes to improve microphase separation, hard domain cohesion, or the ability of the polymer to emulsify or dissolve in polar solvents. The inherent flexibility in polyurethane chemistry allows for an almost endless combination of chain architectures and specific interactions. As a result a wide variety of morphologies have been reported. For PU ionomers, aggregation of ionic groups has been observed within an otherwise one-phase matrix<sup>1,2</sup> or superimposed on the already present microdomain morphology of the nonionic precursor.<sup>3,4</sup>

In a previous study, we reported on the morphology and properties of a series of PU cationomers with pendant trialkylammonium groups.<sup>5</sup> The bulky pendant groups, attached to asymmetric carbon atoms, prevented crystallization in the hard domains. Consequently, little or no microphase separation was evident in un-ionized polymers. On quaternization, dramatic improvements in microphase separation and mechanical properties were observed. The Young's modulus and tensile strength were found to increase by as much as 2 orders of magnitude, and the temperature at which the polymer underwent viscous flow was increased by over 100 °C. Although differential scanning calorimetry

and dynamic mechanical analysis suggested that ionic interactions were the primary driving force for microphase separation in the cationomers, results of small-angle X-ray scattering and tensile testing indicated a lamellar morphology typical of conventional polyurethanes with semicrystalline hard segments. Further, there was no evidence of ionic aggregation within the lamellae. This leads to the question: If ionic functionality is responsible for the tremendous improvement in mechanical properties, but there appears to be no ionic aggregation, what are the specific interactions or physical crosslinks in these materials?

Specific interactions in polyurethanes, particularly hydrogen bonding, have been extensively studied using infrared spectroscopy. Investigators have sought correlations between the type or extent of hydrogen bonding in the polyurethane and its molecular structure,<sup>6–16</sup> degree of microphase separation,<sup>8,11,14,16–22</sup> response to deformation,<sup>10,17,23,24</sup> or thermal transitions.<sup>9,12,14,20,25–28</sup> In conventional segmented polyurethanes, the hydrogen atom of the N–H group in the urethane linkage is the proton donor. A number of proton acceptors are usually present including the urethane carbonyl and alkoxy oxygens and the ester or ether groups which may be incorporated in the soft segments. Hydrogen bonds are indicated by a shift in the stretching frequency of the proton donor or acceptor to lower energy versus the value observed when the group is “free” (i.e., not hydrogen bonded).

Far fewer infrared studies have been performed on PU cationomers. Dietrich *et al.*<sup>29</sup> noted a shift of the N–H band in a segmented PU cationomer to lower frequencies on quaternization and suggested the shift was likely attributable to an increase in the number of hydrogen bonds formed, as Coulombic forces aligned the urethane linkages of neighboring polymer chains. In a study of oligourethanes with terminal amine groups, Lipatov and co-workers<sup>30</sup> reported similar results. In addition to a frequency shift of the N–H band, they observed that on ionization a high fraction of N–H groups remained hydrogen bonded, while most of the carbonyl groups became free. Although quantitative interpretation of the spectra was not attempted, the

\* Author to whom correspondence should be addressed.

† Present address: College of Engineering, University of Delaware, Newark, Delaware 19716.

<sup>®</sup> Abstract published in *Advance ACS Abstracts*, February 1, 1995.

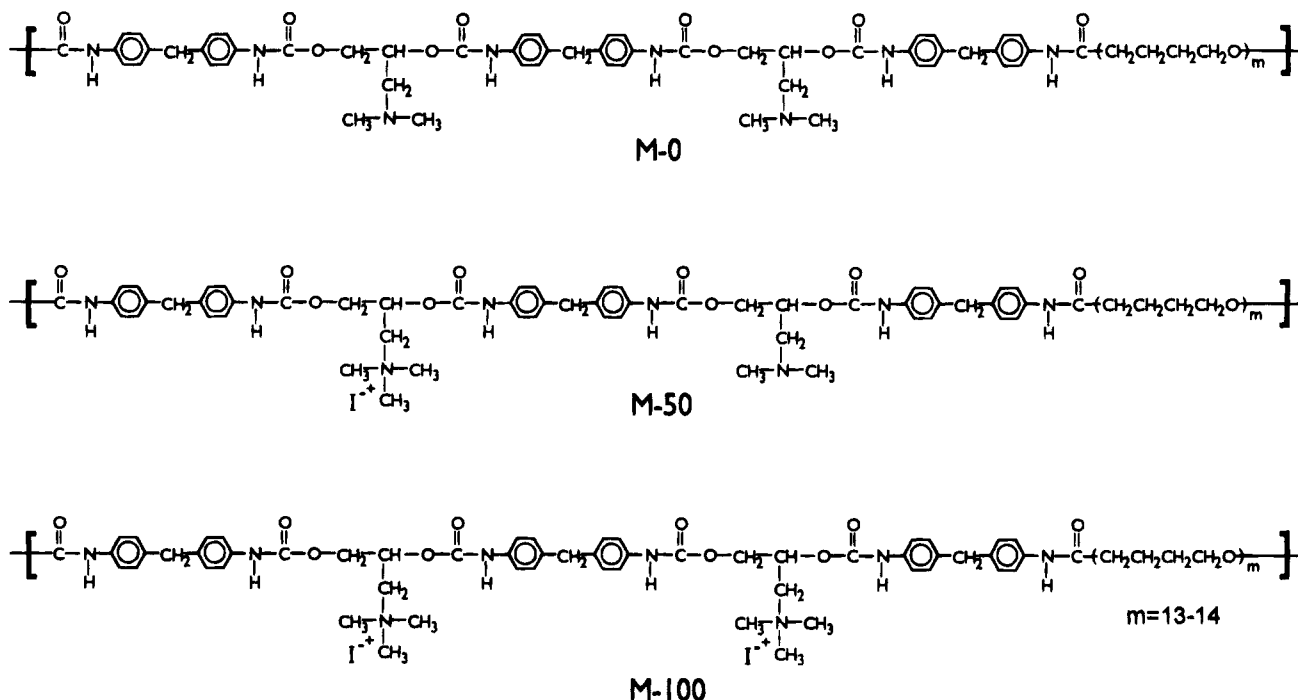


**Figure 1.** Chemical structure of the polyurethane cationomers.

results supported a redistribution of N–H hydrogen bonds from the urethane carbonyl to the iodine ion. In a later paper on multiblock PU cationomers,<sup>31</sup> they postulated a wide array of interactions that included ionic aggregation, N–H to anion bonding, and attractions between the positive charge of the ammonium group and urethane carbonyls. In a number of PU cationomers, Chan and Chen<sup>32–35</sup> noted similar changes in the N–H and carbonyl regions on quaternization. However, interpretation of the carbonyl band was complicated by contributions from the glycolate ion used to neutralize the quaternary amine.

In the present study, Fourier transform infrared (FTIR) temperature studies were completed on a series of polyurethanes with pendant trimethylammonium groups. Spectral deconvolution was used to obtain semiquantitative information on the distribution of hydrogen bonds as a function of temperature and ion content. Such information was used to gain further insight into the nature of the specific interactions, the arrangement of ions within the lamellae, and the mechanism of the upper transition in dynamic mechanical thermal analysis.

## Experimental Section

The materials studied were a series of polyurethane cationomers with a nominal hard-segment content of 50% and a concentration of ionic groups ranging from 0 to 0.88 mequiv/g. The soft segment for all three polymers, whose structures are shown in Figure 1, is poly(tetramethylene oxide) (PTMO;  $M_n = 990$ ). Hard segments consisted of 4,4'-diphenylmethane diisocyanate (MDI) chain-extended with 3-(dimethylamino)-1,2-propanediol (DMP) and/or 3-(trimethylammonio)-1,2-propanediol iodide (TMPI). The polymers were prepared via a two-step polymerization in *N,N*-dimethylacetamide (DMAc) as described previously.<sup>5</sup> Ionic content was varied by adjusting the ratio of DMP and TMPI. Sample nomenclature for the series is M-###, where ### is the mole percent of TMPI as the chain extender. Polymers were solution cast from anhydrous DMAc (Aldrich) into thin films for all analytical tests. Most of the solvent was evaporated with dry air at 50 °C; residual solvent was removed by placing the samples in a vacuum oven at 50–55 °C for 4 days and then at room temperature for 1–3 days.

**Dynamic Mechanical Thermal Analysis (DMTA).** Spectra were collected with a Rheometrics RSA II in autotension mode, with a 120% force for pretension. Temperature steps of 3 °C, with a 0.1 min soak time and a test frequency of 16 Hz, were used over the temperature range of –150 to +175 °C. Approximate sample dimensions were 22.5 × 6.3 × 0.2 mm.

**Thermogravimetric Analysis (TGA).** TGA scans were performed by Betec Laboratory on a DuPont 9900 thermal analysis system. Approximately 25 mg of sample was heated in a nitrogen atmosphere at a rate of 3 °C/min. This rate is virtually identical to that used in DMTA measurements, although the former is a temperature ramp, while the latter is obtained in small temperature steps.

**Infrared Analysis.** Samples for infrared analysis were cast directly onto sodium chloride windows from a 1% (w/v) solution of polymer in DMAc. Film thicknesses were adjusted such that the maximum absorbance of any band was less than 0.7 to be conservatively within the absorbance range where the Beer–Lambert law is valid.<sup>36</sup> Spectra were acquired on either a Mattson Model GL-5020 (Figures 2, 3b, 5, and 7b) or a Nicolet Model 740 FTIR spectrometer using a MCT detector at a resolution of 2 cm<sup>–1</sup>. The number of scans ranged from 64 to 512. Elevated temperature measurements were obtained by placing the polymer/NaCl sample in a well-insulated homemade temperature cell with resistance heaters and NaCl windows. The temperature was measured at the surface of the sample and was controlled to within 0.5 °C using a PID controller tuned to eliminate overshoot. Samples were maintained at the target temperature for 3 min prior to data collection. Additional spectra, taken at times as long as 60 min, were essentially identical, indicating that 3 min was adequate to reach equilibrium conditions.

Prior to quantitative analysis, three different complications in the raw spectra necessitated correction: (i) contributions from water vapor, (ii) extraneous background absorbance, and (iii) changes in sample thickness.

Spectral features attributable to water vapor were evident in some of the data taken at elevated temperatures in spite of the careful drying technique employed. The presence of water is a concern, since it would complicate interpretation of the results if its source were water absorbed in the polymer. Water retention in polyurethanes is well-known, and the extreme hydrophilicity of the polyurethane cationomers used in the present study was previously reported.<sup>37</sup> However, we strongly believe that the source was absorbed/adsorbed water

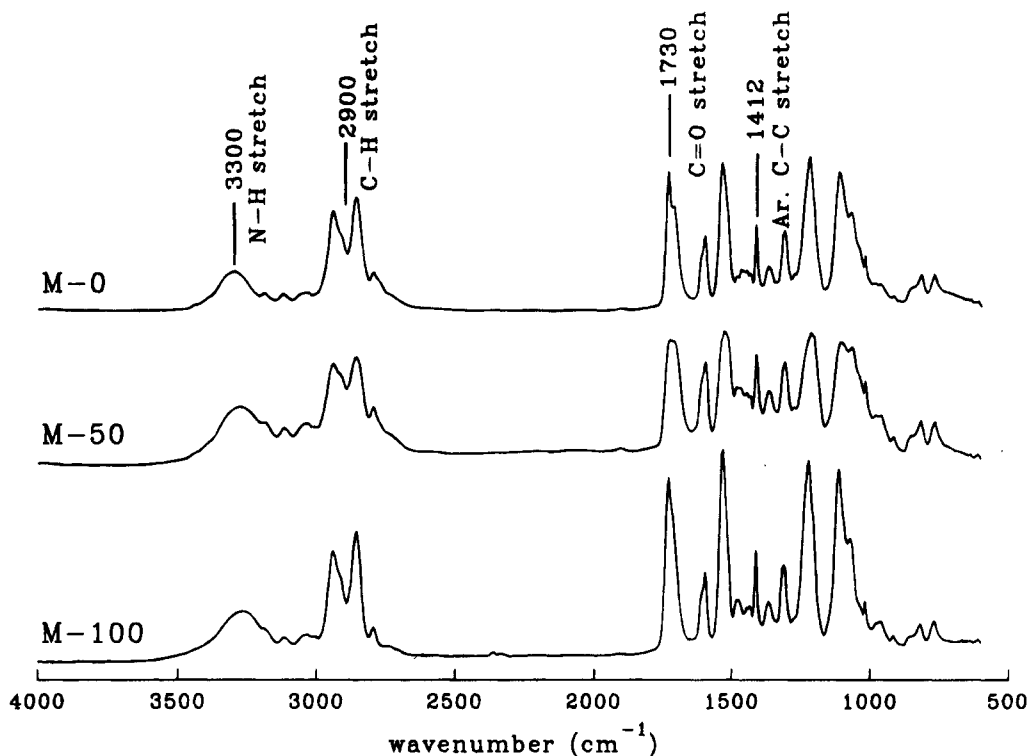


**Figure 2.** Room temperature FTIR spectra of the polyurethane cationomers as a function of ion content.

on components of the heating cell, as water vapor was also evident in spectra obtained at elevated temperatures without a polymer sample.

Extraneous background absorbance can greatly compromise quantitative infrared studies, since any baseline subtraction is an approximation. For this reason only excellent quality spectra, where the baseline was either constant or linear with a slight slope, were retained. A linear baseline through regions of negligible absorbance was subtracted from each spectrum; specifically, a least-squares fit of data between 3800–3700 and 2300–2200  $\text{cm}^{-1}$  was performed.

The final correction to raw spectra was normalization of absorbances for varying sample thickness. This was necessary since all polymer samples were not of the same thickness. Further, the thickness of a given sample usually changed during the course of heating and cooling experiments as a result of viscous flow. To correct for varying sample thickness, the ordinates of all spectra and all reported areas have been normalized to the integrated area between 2980 and 2820  $\text{cm}^{-1}$ . This frequency range contains the strongest of the bands between 3100 and 2700  $\text{cm}^{-1}$  which are associated with symmetric and asymmetric stretches of aliphatic  $\text{CH}_2$  groups. Nearly identical results were obtained using a second band to normalize thickness, namely, the peak absorbance of the aromatic C–C stretch at 1412  $\text{cm}^{-1}$ . Results using the two different bands agreed within approximately 2% in all cases, a negligible error relative to assumptions employed later in band deconvolution.

## Results

Room temperature spectra for the three PU cationomers are shown in Figure 2. Close examination of the spectra reveals that on ionization no new vibrations, only relative changes in intensity or position of bands, are observed. Two main spectral regions are of interest in this study; N–H stretching from 3150 to 3500  $\text{cm}^{-1}$  and the amide I absorption band (commonly referred to as carbonyl stretching) from 1650 to 1800  $\text{cm}^{-1}$ . In this section, the effect of temperature on the two spectral regions is presented. Results are then discussed for each polymer in terms of its chemical structure and morphology.

**N–H Stretching Region.** FTIR spectra of the N–H stretching region, obtained during heating from 30 to 180  $^{\circ}\text{C}$ , are shown for each of the three PU cationomers in Figure 3. Looking first at the room temperature spectrum of sample M-0, one can readily identify at least four bands. The broad absorption centered at approximately 3300  $\text{cm}^{-1}$  is assigned to hydrogen-bonded N–H groups, while the free N–H stretch appears as a small shoulder at 3445  $\text{cm}^{-1}$ . Bands at 3400 and 3180  $\text{cm}^{-1}$  are attributed to overtones of fundamental vibrations in the carbonyl region. Again looking at only room temperature spectra, the hydrogen-bonded band broadens and shifts to lower frequencies with increasing ion content. This shift in position of the band maximum corresponds to an increase in the average strength of the hydrogen bond at higher ion concentrations.

For the unquaternized polymer M-0, Figure 3a shows that the band associated with hydrogen-bonded N–H groups broadens and shifts to higher frequency as the temperature increases. A substantial decrease in the band area is also evident. Similar trends have been observed in model polyurethane hard segments<sup>20,38</sup> and in segmented polyurethanes with amorphous<sup>26</sup> or semicrystalline<sup>24–26,28</sup> hard segments. A clearly different behavior is observed in the quaternized polymers, M-50 and M-100, of Figure 3b,c. At intermediate temperatures, one can see that the broad band earlier attributed to hydrogen-bonded N–H groups is in fact two bands. The position of the band at higher wavenumbers matches closely that observed in a variety of nonionic polyurethanes and will be referred to hereafter as a “traditional” hydrogen bond. The second band, lower in frequency by some 50–100  $\text{cm}^{-1}$ , is assigned to N–H stretching where the N–H groups are hydrogen bonded to the iodine anion. A lower frequency vibration is consistent with this assignment, since a greater hydrogen bond strength would be expected with a halide ion as compared to carbonyls or ethers. An analogous shift has been reported for hydrogen bonding of alcohols

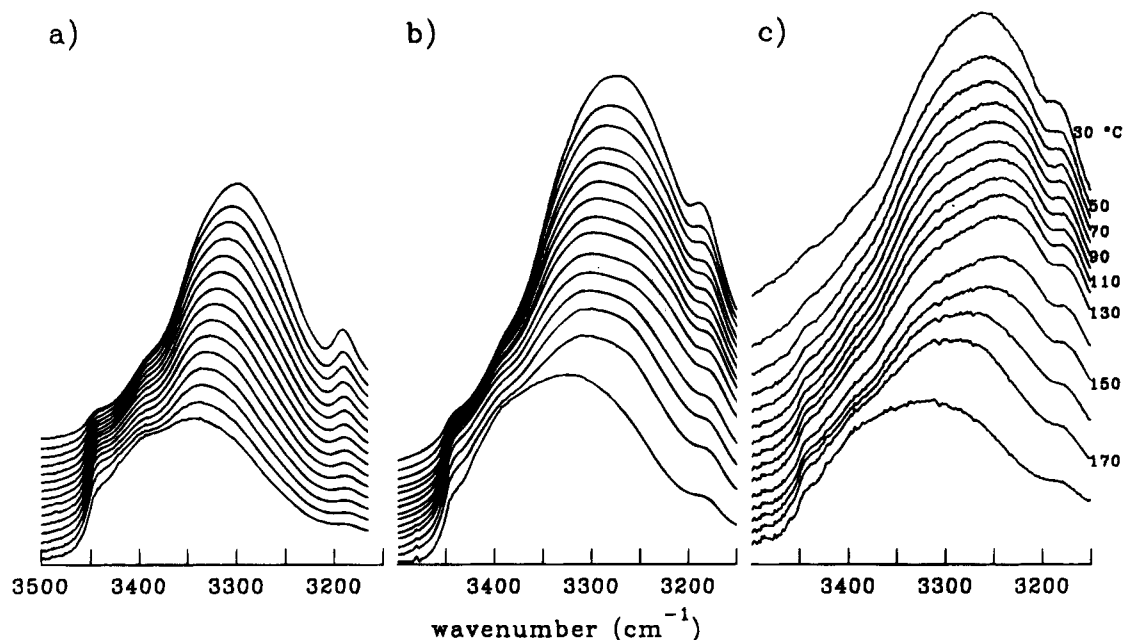


**Figure 3.** FTIR spectra in the N–H stretching region for (a) M-0, (b) M-50, and (c) M-100 as a function of increasing temperature from 30 to 180 °C.

**Table 1. Summary of Relevant Band Assignments**

assignment	frequency (cm <sup>-1</sup> )	occurrence
N–H stretching region	~3150–3500	
free N–H	3445	M-0, M-50, M-100
N–H bonded to anion	3260	M-50, M-100
N–H bonded to ether <sup>a</sup>	3300	M-0
N–H bonded to carbonyl	3326	M-0, M-50, M-100
C=O stretching region	~1650–1800	
free C=O	1736	M-0, M-50, M-100
hydrogen-bonded C=O	1710	M-0, M-50, M-100
aliphatic C–H stretching	2820–2980 <sup>b</sup>	
aromatic C–C stretching	1412	

<sup>a</sup> Band likely comprised of N–H bonded to ether and carbonyl groups. <sup>b</sup> Arbitrarily defined limits of region for use in normalization.

to low molecular weight compounds containing halide ions.<sup>39,40</sup> Band assignments for the N–H region (and the carbonyl region discussed below) are summarized in Table 1.

Reversibility of the results of Figure 3 was tested by heating samples to 180 °C and acquiring spectra on cooling. As shown in Figure 4 for M-100, the process is clearly not reversible from 180 °C. In fact, the N–H region of the final spectrum at 30 °C resembles an initial spectrum of M-0 more closely than an initial spectrum of M-100. Not surprisingly, dequaternization was verified in the PU cationomers at elevated temperatures through measurement of the iodine content, although weight loss measurements greater than theoretical indicate other modes of decomposition also occur.<sup>41</sup> Thermogravimetric analysis indicated a 2% weight loss for the cationomer M-100 up to 200 °C. Since the time scale of the FTIR cooling experiment and TGA are comparable, the dramatic difference between the initial and final spectra of Figure 4 is therefore likely accompanied by a loss of no more than 15% of the ammonium groups. Through trial and error, the maximum temperature for complete reversibility of the observed changes in infrared spectra during heating was determined. As shown in Figure 5, spectra obtained during cooling the PU cationomers from 140 °C closely match those obtained during heating at all temperatures.

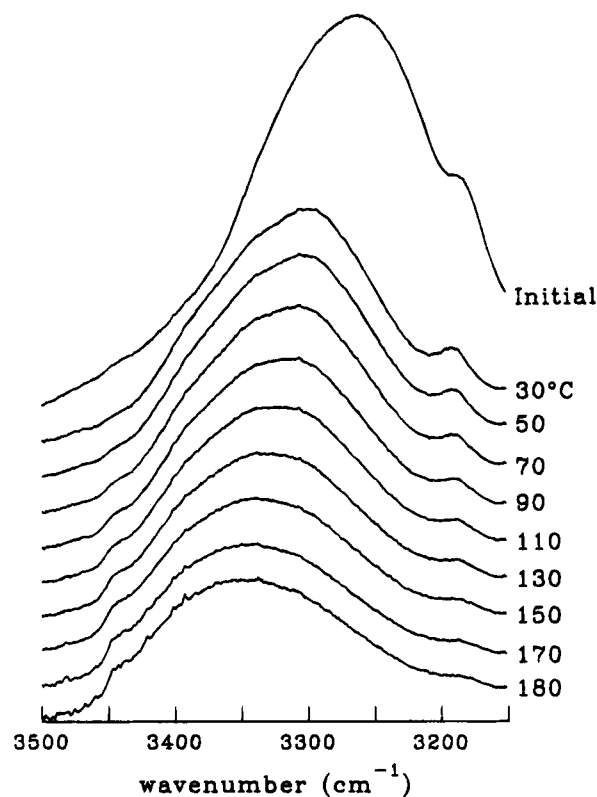


**Figure 4.** N–H stretching region of M-100 recorded as a function of decreasing temperature from 180 °C. An “Initial” spectrum of M-100, taken at room temperature prior to heating, is included for comparison.

Deconvolution of the N–H stretching region was completed on spectra up to 140 °C using the curve-fitting program PeakFit available from Jandel Scientific. Limits of the curve fit were set at 3250 and 3500 cm<sup>-1</sup> for M-0, and 3210 and 3500 cm<sup>-1</sup> for M-50 and M-100, to avoid the low-frequency overtone vibration at 3180 cm<sup>-1</sup>; Gaussian functions were assumed for all N–H stretching bands. The PeakFit program determines the best fit of the experimental data by varying the frequency  $\nu$ , width at half-height fwhm, and area of each band using the Marquardt–Levenberg algorithm. Co-

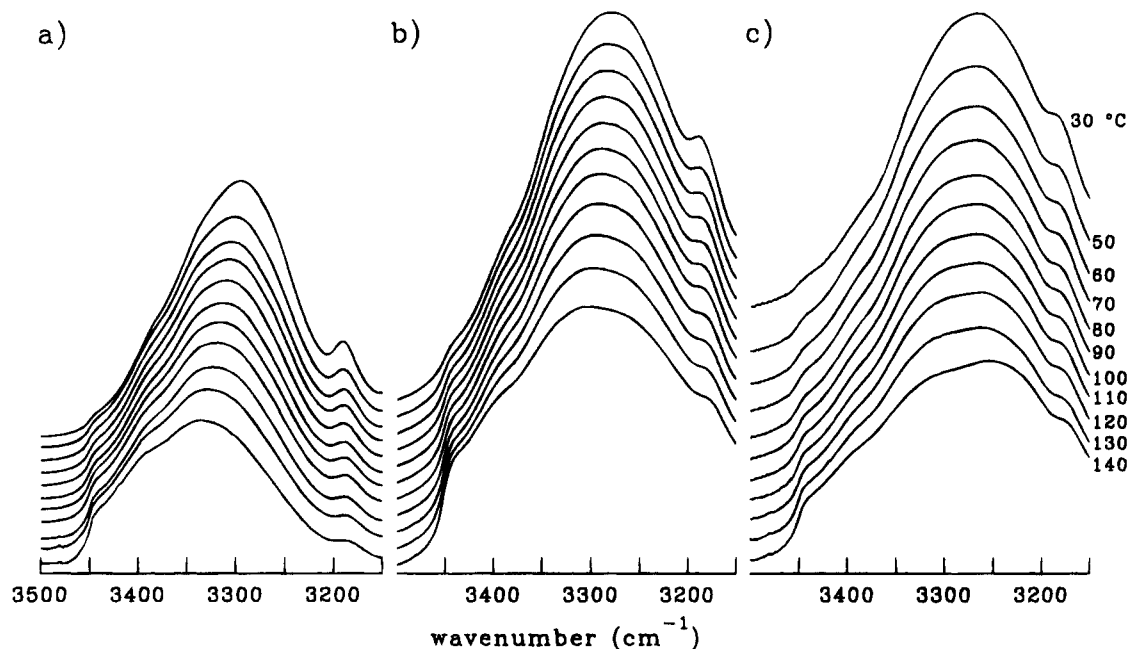


Figure 5. Same as Figure 3, except spectra were recorded as a function of decreasing temperature from 140 °C.

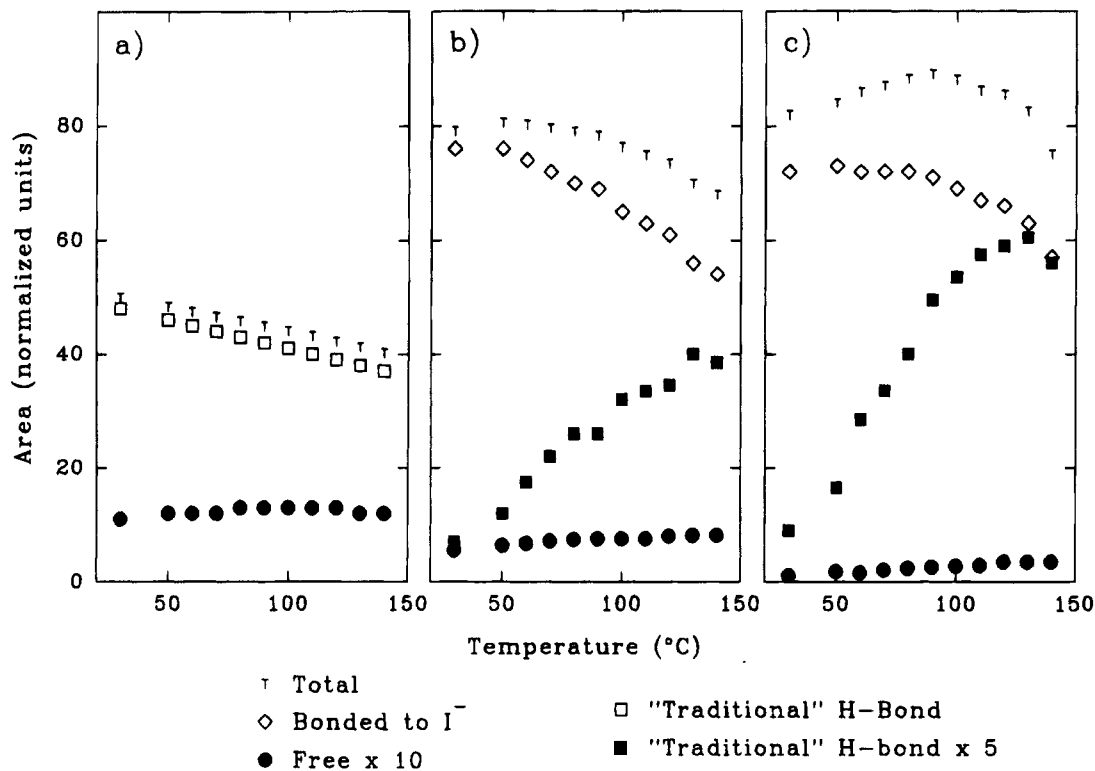
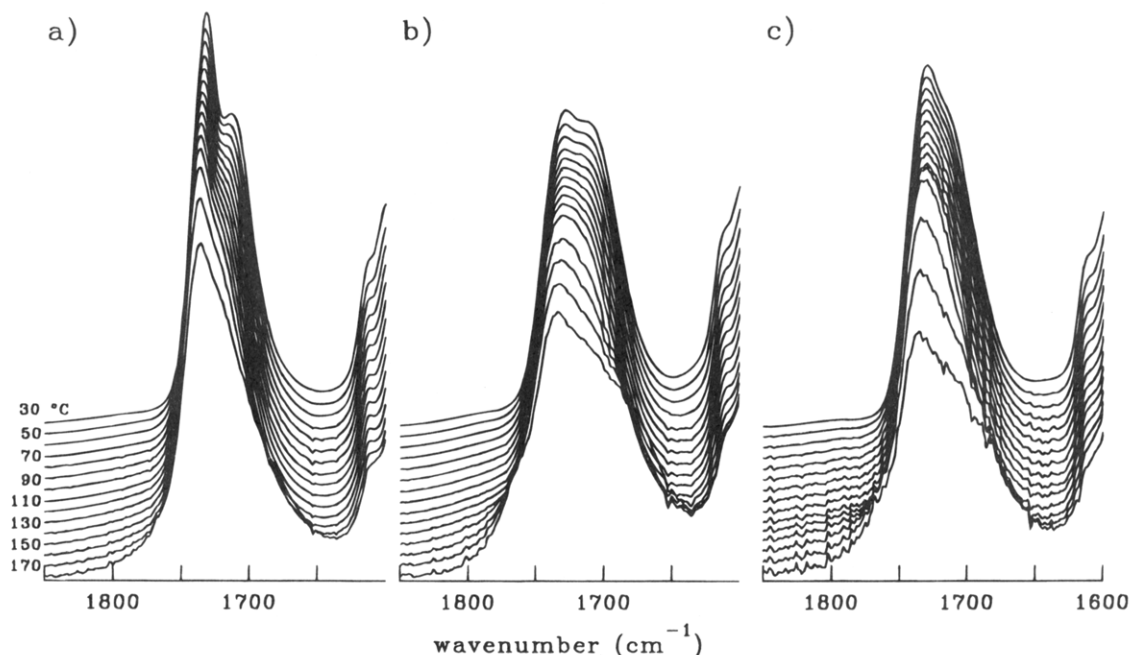


Figure 6. Normalized areas of assigned bands in the N-H stretching region as a function of temperature from 30 to 140 °C. Note that areas for two of the bands have been multiplied by constants to improve intelligibility.

efficients of determination were greater than 0.999 for all three samples at all temperatures. In spite of the excellent analytical fits, quantifying the distribution of the different types of N-H groups is not possible. The absorptivity coefficient,  $\alpha$ , of the N-H and O-H stretching vibrations has been shown to be a strong function of frequency.<sup>38,42-45</sup> In the present study, the absorptivity coefficient likely varies enough across the frequency range of some bands that a proper shape cannot be assigned, with the result that peak deconvolution may be invalid. In fact, we contemplated not curve fitting the N-H region at all, since the reader may be tempted to "use the numbers" to obtain quantitative

information. Hopefully the cautionary discussion above is sufficient to prevent such overinterpretation of the data. With the extensive overlap of bands in the N-H stretching region, we feel that curve fitting aids the eye of the reader in seeing trends.

Optimum parameters for curve fitting the N-H stretching region of the PU cationomers from 30 to 140 °C are available in table form as supplementary data, with area changes displayed graphically in Figure 6. The area of the free N-H band is directly related to the number or concentration (but NOT fraction) of free N-H groups, since the frequency of the vibration is nearly constant for all samples at all temperatures.



**Figure 7.** FTIR spectra in the carbonyl stretching region for (a) M-0, (b) M-50, and (c) M-100 as a function of increasing temperature from 30 to 180 °C.

However, on the basis of the uncertainties in area determination, we believe the relative error in area is on the order of 50% and therefore would not attempt to state any trend in the number of free N-H groups with temperature for any of the PU cationomers. On the other hand, the observed trend of decreasing concentration of free N-H groups with increasing ionization level appears to be real. This is consistent with the greater number of ions available as proton acceptors.

As the temperature is increased from 30 to 140 °C, the frequency of the "traditional" hydrogen-bonded band for all three polymers increases regularly, indicating a decrease in the average hydrogen bond strength with increasing temperature. The area of the "traditional" hydrogen-bonded N-H stretching band for sample M-0 decreases by about 25% as the temperature is increased from 30 to 140 °C. It is difficult to say whether or not this corresponds to a decrease in the number of hydrogen-bonded N-H groups, since the absorptivity coefficient decreases with increasing frequency as the temperature is raised. In contrast, the band area for the quaternized polymers increases roughly 6-fold from 30 to 140 °C. This change can be conclusively attributed to an increase in the concentration of N-H groups hydrogen bonded to traditional proton acceptors, since the absorptivity coefficient for the band is decreasing as its area increases.

At the same time, one can see that as the temperature is increased the area of the band assigned to N-H groups hydrogen bonded to the anion decreases. As with the "traditional" hydrogen-bonded N-H band of M-50 and M-100, the trend in band area with temperature is in the opposite direction of the trend for the absorptivity coefficient, so we know this corresponds to a decrease in the number of anion-bonded N-H groups. In other words, as the temperature is increased, there is a shift in hydrogen bonding of the N-H groups from the anion to traditional proton acceptors.

**C=O Stretching Region.** FTIR spectra of the carbonyl stretching region, taken during heating from 30 to 180 °C, are shown for each of the three PU cationomers in Figure 7. All spectra appear to be

composed of two bands, although there is considerable overlap at higher temperatures. The narrower band centered at about 1736  $\text{cm}^{-1}$  is assigned to stretching of free carbonyl groups, while the band at approximately 1712  $\text{cm}^{-1}$  is attributed to hydrogen-bonded carbonyl groups. These positions are very close to those obtained by Boyarchuk and co-workers<sup>46</sup> for urethane elastomers in dilute and concentrated carbon tetrachloride solutions, respectively. A number of previous investigators have assigned the carbonyl stretch at roughly 1712  $\text{cm}^{-1}$  to hydrogen bonding in disordered regions (i.e., urethane linkages of interfacial regions or "dissolved" in the soft phase).<sup>12,38,47</sup> In these same studies, a third carbonyl band at a lower frequency ranging from 1684 to 1702  $\text{cm}^{-1}$  has been attributed to stronger hydrogen bonds in ordered or crystalline regions. Quite expectedly, an ordered hydrogen-bonded carbonyl band is not observed in the amorphous materials of the present study. Zharkov *et al.*<sup>48</sup> recently suggested that the amide I band of segmented polyurethanes consisted of no less than five absorption bands, free carbonyls at 1740 and 1730  $\text{cm}^{-1}$ , and hydrogen-bonded carbonyls at 1725, 1713, and 1702  $\text{cm}^{-1}$ . Discrimination of free and hydrogen-bonded carbonyls was based on the type of proton acceptor (if any) to which the neighboring urethane N-H group is associated. It is certainly possible that the two carbonyl bands assumed in the present study are combinations of bands identified by Zharkov and co-workers; however, the spectra of the PU cationomers showed no obvious traits which warranted such a differentiation. Further, it appears that possible multicomponent bands would not compromise a more simplified division of "free" and "hydrogen-bonded" groups.

The carbonyl region was also deconvoluted using the commercial software program PeakFit. Limits of the curve fit were set at 1685 and 1775  $\text{cm}^{-1}$  for all three polymers, with best fits obtained using a Gaussian function for the free carbonyl and a Gaussian-Lorentzian sum for the hydrogen-bonded carbonyl. Following a trial iteration of curve fitting in which all parameters were allowed to float, the Gaussian component of the

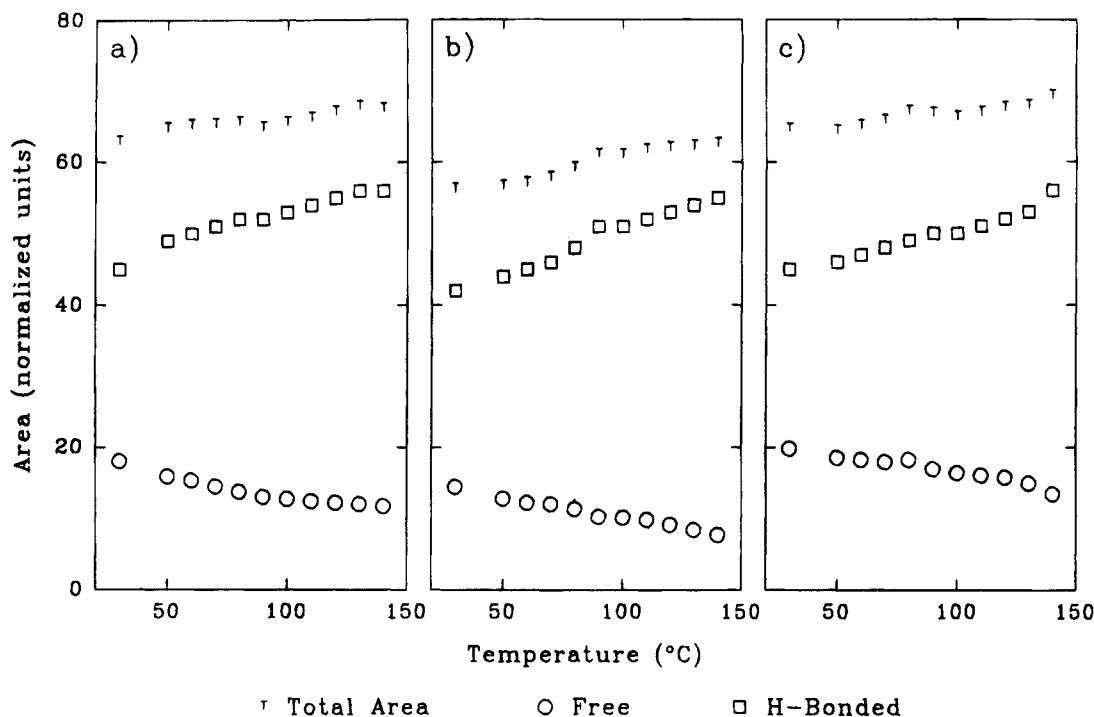


**Figure 8.** Normalized areas of bands assigned to free and hydrogen-bonded carbonyl groups as a function of temperature from 30 to 140 °C.

hydrogen-bonded carbonyl was fixed at the average value of 80%. Excellent analytical fits were consistently obtained, with coefficients of determination greater than 0.999 for all three samples at all temperatures.

Optimum parameters for curve fitting the carbonyl stretching region, again limited to a maximum of 140 °C to avoid results which might be complicated by dequaternization, are also available as supplementary data. Smooth trends with temperature, and consistency of results for the three polyurethanes, impart some level of confidence in the results. The frequency of the free carbonyl band is nearly constant ( $1737 \pm 2 \text{ cm}^{-1}$ ) over the entire experimental range of temperature and ion content, while the hydrogen-bonded carbonyl band shifts regularly to higher frequency from room temperature to 140 °C. Like the N–H stretching region, this increase in frequency corresponds to a decrease in the average hydrogen bond strength with increasing temperature.

In all three polymers the area of the free carbonyl band ( $A_F$ ) shown in Figure 8 decreases almost linearly with increasing temperature. A parallel increase in area with temperature is observed for the hydrogen-bonded band ( $A_B$ ). As compared to the N–H stretching region, the frequencies of the vibrations in the carbonyl stretching region do not shift as much with temperature, and the absorptivity coefficient is not as strong a function of  $\nu$ . The band area changes of the carbonyl region are therefore directly related to an increase in the fraction of hydrogen-bonded carbonyls with increasing temperature. This trend in the number of hydrogen-bonded groups with temperature is counterintuitive and in the opposite direction of all (to the best of the authors' knowledge) previously reported infrared temperature studies on polyurethanes with either amorphous,<sup>27</sup> mesogenic,<sup>12</sup> or semicrystalline<sup>8,20,24,28,38</sup> hard segments. In Figure 8, one can also see that the total area of the carbonyl region ( $A_T$ ) increases with increasing temperature. Since the total concentration of carbonyl groups is constant for each sample, the changes in the total area are caused by a greater absorptivity coefficient for the

hydrogen-bonded carbonyl ( $\alpha_B$ ) than for free carbonyls ( $\alpha_F$ ). Although this difference in  $\alpha$  complicates the calculation of the distribution of free and hydrogen-bonded carbonyl groups, the fractions can be approximated by the following analysis. The total area as a function of temperature  $T$  is given by:

$$A_T(T) = A_B(T) + A_F(T) \quad (1)$$

Substituting the Beer–Lambert law,  $A_i = \alpha_i C_i L$ , for the integrated absorbance of each band as a function of the total concentration of carbonyl groups  $C$  and path length  $L$ ,

$$A_T(T) = CL[\alpha_B(T) X_B(T) + \alpha_F(T) (1 - X_B(T))] \quad (2)$$

where  $X_B(T)$  is the fraction of hydrogen-bonded carbonyls. Since the results have already been normalized such that the  $CL$  product is a constant,  $A_T(T)$  is constant only if  $\alpha_B(T) = \alpha_F(T)$ . In the present case  $A_T(T)$  is not constant. However, we can define  $r(T) = \alpha_B(T)/\alpha_F(T)$ ,  $A_F^*(T) = r(T) A_F(T)$  and  $A_T^*(T) = A_B(T) + A_F^*(T)$  such that:

$$A_T^*(T) = A_B(T) + r(T) A_F(T) = CL\alpha_B(T) \quad (3)$$

If we now assume that  $\alpha_B$  and  $\alpha_F$  are constant with temperature, then according to eq 3  $A_T^*$  will also be a constant, with the fractions of free and hydrogen-bonded groups given by  $X_F(T) = A_F^*(T)/A_T^*$  and  $X_B(T) = A_B(T)/A_T^*$ .

The ratio of the absorptivity coefficients  $r$  for each polymer can be obtained via a linear least-squares fit of  $A_B(T)$  versus  $A_F(T)$  as indicated in eq 3. Results of the analysis are displayed in Figure 9, with the adjusted areas  $A_F^*$  and  $A_T^*$  determined from the average value of  $r = 1.88 \pm 0.29$  for the three polymers. All values of  $A_T^*$  are within 2% of the average for each sample indicated by a short-dashed line. The occurrence of a near-constant adjusted total area, using a single value



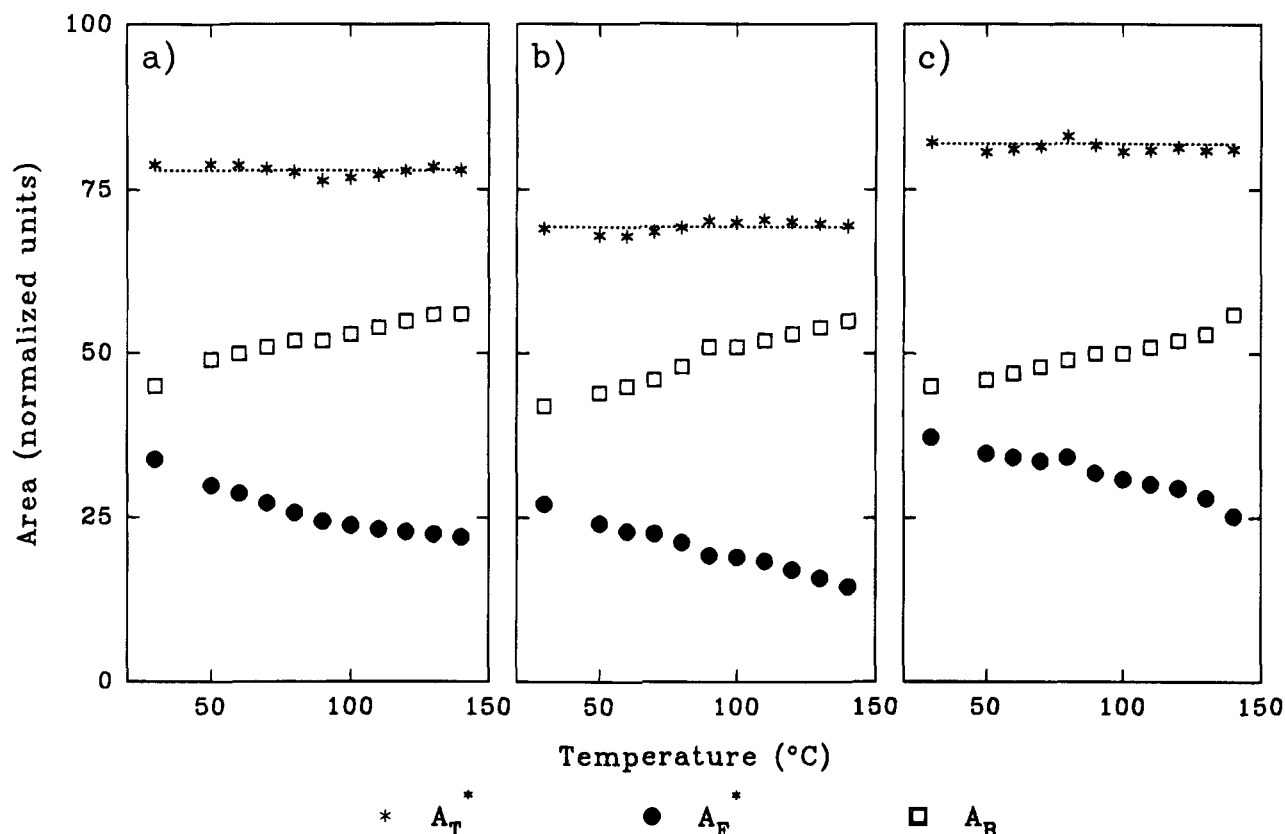
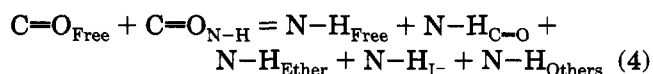


**Figure 9.** Adjustment of areas in Figure 8 for the inequality of the absorptivity coefficients of the free and hydrogen-bonded carbonyl bands.

of  $r = 1.88$  for three polymers which contain widely differing ion contents, bestows some credibility to the technique. Further, the average ratio of absorptivity coefficients is in reasonable agreement with the value  $r = 1.71$  estimated by Coleman and co-workers<sup>38</sup> for a semicrystalline polyurethane homopolymer. From the results of Figure 9, the fraction of free carbonyls at room temperature is 0.43 for M-0, 0.39 for M-50, and 0.45 for M-100. A steady decrease in  $X_F$  is evident for all three polymers with increasing temperature, with the fraction of free carbonyls at 140 °C being approximately 0.28 for M-0, 0.21 for M-50, and 0.31 for M-100. Although comparable trends in the distribution of free and hydrogen-bonded carbonyl groups with temperature are observed for all three PU cationomers, and indeed the actual fractions at all temperatures are strikingly similar, very different mechanisms are involved for the two quaternized polyurethanes versus sample M-0.

## Discussion

Results of the FTIR temperature experiments are discussed for each of the three PU cationomers in terms of its chemical structure, morphology, and thermomechanical properties. For polymers M-0 and M-100, a rough approximation of the distribution of various hydrogen bonds is sought using mass balances and the calculated fractions of free and hydrogen-bonded carbonyl groups. Since the total numbers of N-H and C=O groups are equal, the following equality can be written:



Known contributions to  $\text{N-H}_{\text{Others}}$  include hydrogen

bonding to urethane alkoxy oxygens and  $\pi$  orbitals of aromatic rings. Direct calculation of this contribution would of course be beneficial but is unrealistic in the present investigation due to the complexity of the system. Results from previous studies<sup>27,38,49</sup> suggest that  $\text{N-H}_{\text{others}}$  is on the order of 10% for a wide variety of polyurethanes of varying chemistry and morphology.

**Polymer M-0.** At room temperature, we estimated that 57% of the urethane carbonyls in sample M-0 were hydrogen bonded. Since  $\text{N-H}_{\text{I-}}$  is zero for the unquaternized polymer, eq 4 indicates that 43% of N-H groups are either free or bonded to ethers and "others". Although the fraction of free N-H groups cannot be calculated accurately, previous estimates<sup>8,28,38,50</sup> for  $\alpha_B/\alpha_F$  between 3.1 and 5.6 suggest a number far less than 43%. This implies that a substantial fraction of N-H groups in M-0 are hydrogen bonded to ethers of the PTMO soft segment. Such a result is not surprising since our previous study<sup>5</sup> showed that this polymer is primarily a homogeneous hard-segment/soft-segment material. According to the stoichiometry shown in Figure 1, there are roughly 2 times as many ether groups available as carbonyl groups if the polymer lacks microphase separation. Further evidence for hydrogen bonding to ethers is obtained from the frequency of the N-H stretching vibration assigned to "traditional" hydrogen bonding. In sample M-0  $\nu$  is 3300  $\text{cm}^{-1}$  at room temperature, as compared to 3326  $\text{cm}^{-1}$  in both M-50 and M-100. Using infrared spectra of segmented polyurethanes with monodisperse hard segments of varying length, Christenson and co-workers<sup>11</sup> assigned N-H stretches at 3321–3328 and 3258–3265  $\text{cm}^{-1}$  to N-H groups hydrogen bonded to urethane carbonyls and polyol ethers, respectively. Through FTIR temperature studies, Lee *et al.*<sup>21</sup> also associated a band at



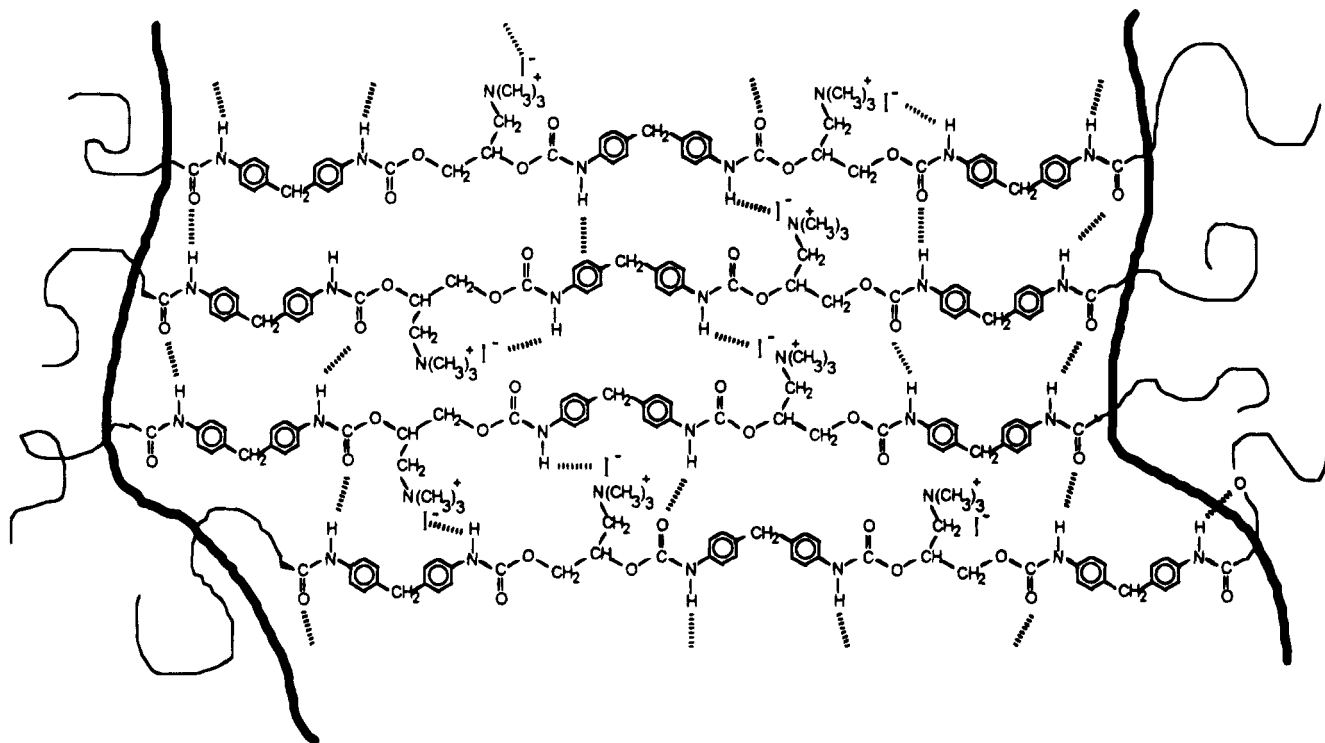
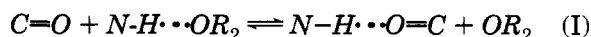


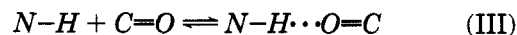
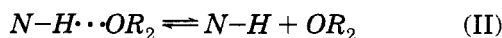
**Figure 10.** Schematic of hydrogen bonding, and plausible packing arrangement, in polyurethane cationomer hard domains.

3295  $\text{cm}^{-1}$  with N-H bonded to ethers in microphase-separated polyurethanes. For sample M-0, we might therefore expect that the "traditional" hydrogen-bonded band at 3300  $\text{cm}^{-1}$  is a superposition of broad distributions attributable to N-H groups hydrogen bonded to ethers and carbonyls.

As the unquaternized polymer is heated from 30 to 140  $^{\circ}\text{C}$ , we estimated that the fraction of hydrogen-bonded carbonyls increased from 0.57 to 0.72. If the only interactions present were between N-H and carbonyl groups, the fraction of free N-H groups would have to decrease by 0.15 over the same temperature range. Although the trend in the number of free N-H groups with temperature is not known, a decrease of 0.15 in the fraction of free N-H groups would certainly be evident and outside the range of experimental error, since probably no more than 15% of the N-H groups are free at 30  $^{\circ}\text{C}$ . Further, a transformation of free to hydrogen-bonded N-H groups with *increasing* temperature is inconsistent with equilibrium considerations. This discrepancy can be explained by again considering the bonding of N-H groups to ethers of the soft segment. As temperature is increased, the fraction of N-H groups hydrogen bonded to ether oxygens decreases, while the fraction hydrogen bonded to carbonyl groups increases. This redistribution of N-H bonding can be explained by the simplified picture of the competing equilibrium outlined below; consider the reaction



This can be represented by a sum of the primary reactions II and III



The greater frequency shift for N-H groups hydrogen bonded to ether oxygens, as compared to that for carbonyls, is evidence that the enthalpy of reaction II is greater than the enthalpy of reaction III. Hence, reaction I is endothermic, and the equilibrium position shifts to the right as temperature is increased.

**Polymer M-100.** Approximately 55% of the carbonyl groups in the fully ionized polymer are hydrogen bonded at room temperature. Although we cannot determine the fraction of free N-H groups with confidence,  $\text{N}-\text{H}_{\text{Free}}$  appears negligible from the following crude analysis. The area of the free N-H stretching band is 0.13% of the total area of the N-H region. From the total areas of Figure 6, we know that the average absorptivity coefficient for the N-H stretching region,  $\alpha_{\text{ave}}$ , is around 1.6 times greater for M-100 than M-0 at 30  $^{\circ}\text{C}$ . Using a conservative value of  $\alpha_{\text{B}}/\alpha_{\text{F}} = 6.2$  for the traditional hydrogen bond, then  $\alpha_{\text{ave}}/\alpha_{\text{F}}$  is about 10 for M-100, and just over 1% of the N-H groups are free. Even if the area of the free N-H band (or our estimate of the ratio of absorptivity coefficients) is off by a factor of 2 or 3,  $\text{N}-\text{H}_{\text{Free}}$  is only a few percent. We will further assume that  $\text{N}-\text{H}_{\text{Ether}}$  is comparatively small, since our previous findings indicate little microphase mixing in the fully quaternized PU.<sup>5</sup> If from these arguments we simply estimate at this point that the sum  $\text{N}-\text{H}_{\text{Free}} + \text{N}-\text{H}_{\text{Ether}} + \text{N}-\text{H}_{\text{Others}}$  in eq 4 is 15%, then roughly 30% of the N-H groups are hydrogen bonded to the anions. Since the ratio of N-H groups to iodine atoms in M-100 (see Figure 1) is 3:1, approximately one N-H group is hydrogen bonded to each anion. With no crystalline order in the hard domains, a loose arrangement of the hard segments with a number of possible interactions might be expected, as schematically depicted in Figure 10. Such an arrangement, with a large number of relatively strong N-H to anion interchain associations, can satisfactorily explain the tremendous increase in

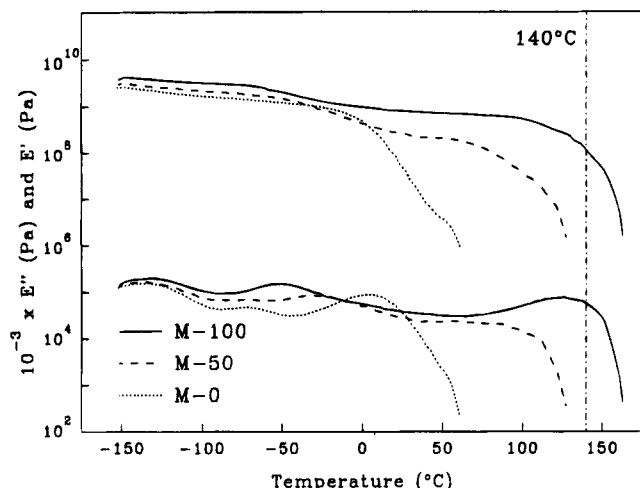


**Figure 11.**  $E'$  and  $E''$  for the three polyurethane cationomers. The vertical dot-dashed line at 140 °C demarcates the approximate maximum temperature at which the infrared spectra are reversible.

tensile properties of these materials on ionization.<sup>5</sup> An arrangement like Figure 10 is also consistent with our earlier observation that no small-angle X-ray scattering peak exists that is attributable to ionic aggregation within the hard domains.<sup>5</sup> If most or all of the iodine atoms are "coupled" to N-H groups, steric restrictions would reduce the likelihood of the ammonium groups aggregating.

When the temperature of M-100 is increased from 30 to 140 °C, the fraction of hydrogen-bonded carbonyls increases from approximately 0.55 to 0.69. In the N-H stretching region, a parallel increase in the fraction of N-H groups hydrogen bonded to carbonyls is observed, while the concentration of N-H groups hydrogen bonded to iodine atoms decreases. Although we can not quantify the trends in the N-H region, the results conclusively indicate a shift in the distribution of N-H hydrogen bonding from the anions to carbonyls with increasing temperature. The results of Figure 5c show that the process is reversible to at least 140 °C, just above the upper transition in the DMTA scan of Figure 11. An analogous explanation to reactions I-III can be given for the shift in N-H bonding at elevated temperatures, since the frequency of the anion-bonded N-H stretching vibration is also lower than that for N-H groups hydrogen bonded to carbonyls.

**Polymer M-50.** Our previous investigation of the 50% quaternized polymer suggested a microphase-separated morphology, with considerable mixing of the mixing of the domains.<sup>5</sup> This prohibits even a crude mass balance like that employed for M-0 or M-100, since eq 4 contains too many unknown terms. In spite of this limitation, some important observations can still be made. First, sample M-50 again shows an increase in the number of hydrogen-bonded carbonyls on heating. Fractions of 0.61 at room temperature and 0.79 at 140 °C are somewhat higher than those for the fully ionized cationomer, an outcome that might be expected since fewer anions are available for bonding to N-H groups in the lower ion content PU. Second, a shift in N-H bonding from the iodine atoms to the carbonyl groups again appears to be the most prominent change on heating, confirming the results of sample M-100. Finally, since the changes are reversible to at least 140 °C and the upper DMTA transition of M-50 is well below this temperature, we can conclusively state that the

viscous flow transition of Figure 11 is also reversible and therefore not caused by dequaternization. In fact, since our evidence suggests that the interchain N-H to anion bonds are the primary interaction which "holds the polymer together", the flow transition is likely a direct consequence of the observed change in N-H bonding at elevated temperatures. We could not make this statement from the results for M-100, where flow and dequaternization (although slight) occur in the same temperature regime.

## Conclusions

The carbonyl stretching region of the infrared spectra of all three polyurethanes displays two bands, attributed to hydrogen-bonded and free carbonyl groups. For sample M-0, the N-H stretching region contains bands assigned to free and traditional hydrogen-bonded N-H groups. The unquaternized sample is not microphase separated, and thus the traditional hydrogen-bonded band likely results from N-H stretching vibrations where both urethane carbonyls and soft-segment ethers are the proton acceptors. In the N-H region of the infrared spectra of the quaternized polyurethanes M-50 and M-100, most of the traditional proton acceptors are urethane carbonyls, since these materials are microphase separated. An additional N-H stretching band, assigned to N-H groups hydrogen bonded to the anions, is also observed. The N-H to anion bond is stronger than the traditional hydrogen bond, and these interchain ties are apparently the specific interaction responsible for the microphase separation and excellent mechanical properties of the PU cationomers. A semi-quantitative N-H group balance for the fully ionized cationomer suggests that roughly one N-H group is bonded to each anion; aggregation of ionic groups within the hard domains is therefore unlikely, though not precluded.

In all three polymers, the fraction of free carbonyl groups decreases with increasing temperature. This trend is in the opposite direction of conventional polyurethanes with semicrystalline hard segments. A redistribution of N-H hydrogen bonding on heating, from the ether groups to urethane carbonyls, is proposed to explain this result for the unquaternized PU. In M-50 and M-100, a similar change occurs with the hydrogen bonding of N-H groups shifting from the anion to carbonyl groups with increasing temperature. Both events are fully reversible to a maximum temperature of approximately 140 °C, beyond which dequaternization of the ammonium groups becomes significant. Although there are no obvious transitions in the infrared temperature spectra which directly correlate with the upper transition in dynamic mechanical thermal analysis spectra, we believe that the flow transition in the PU cationomers is associated with this steady shift in N-H bonding from the anion to carbonyl groups.

**Acknowledgments.** Research support from the U.S. Department of Energy under Grant DE-FG02-88ER-45370 and the National Science Foundation through Grant DMR-90-16959 is gratefully acknowledged. We thank Prof. Robert McMahon and his research group for the use of their Nicolet FTIR while our new spectrometer was on order and Todd C. Scheele for his assistance in sample preparation and data analysis. R.J.G. also acknowledges the support of the Department of Defense through the National Defense Science and Engineering Graduate Fellowship program.

**Supplementary Material Available:** Optimum parameters from deconvolution of the N-H and C=O stretching regions are available as tables (2 pages). Ordering information is given on any current masthead page.

## References and Notes

- (1) Ding, Y. S.; Register, R. A.; Yang, C. Z.; Cooper, S. L. *Polymer* **1989**, *30*, 1213.
- (2) Visser, S. A.; Cooper, S. L. *Polymer* **1992**, *33*, 3790.
- (3) Lipatov, Y. S.; Shtompel, V. I.; Vilenskii, V. A.; Kercha, Y. Y.; Shrubovich, V. A.; Shevchenko, V. V. *Polym. Sci. USSR* **1987**, *29*, 606.
- (4) Yang, C. Z.; Grasel, T. G.; Bell, J. L.; Register, R. A.; Cooper, S. L. *J. Polym. Sci., Part B: Polym. Phys.* **1991**, *29*, 581.
- (5) Goddard, R. J.; Cooper, S. L. *J. Polym. Sci., Part B: Polym. Phys.* **1994**, *32*, 1557.
- (6) Trifan, D. S.; Terenzi, J. F. *J. Polym. Sci.* **1958**, *28*, 443.
- (7) Tanaka, T.; Yokoyama, T.; Yamaguchi, Y. *J. Polym. Sci., Polym. Chem. Ed.* **1968**, *6*, 2153.
- (8) Srichatrapimuk, V. W.; Cooper, S. L. *J. Macromol. Sci., Phys.* **1978**, *B15*, 267.
- (9) Brunette, C. M.; Hsu, S. L.; MacKnight, W. J. *Macromolecules* **1982**, *15*, 71.
- (10) Lin, S. B.; Hwang, K. S.; Tsay, S. Y.; Cooper, S. L. *Colloid Polym. Sci.* **1985**, *263*, 128.
- (11) Christenson, C. P.; Harthcock, M. A.; Meadows, M. D.; Spell, H. L.; Howard, W. L.; Creswick, M. W.; Guerra, R. E.; Turner, R. B. *J. Polym. Sci., Part B: Polym. Phys.* **1986**, *24*, 1401.
- (12) Pollack, S. K.; Shen, D. Y.; Hsu, S. L.; Wang, Q.; Stidham, H. D. *Macromolecules* **1989**, *22*, 551.
- (13) Harthcock, M. A. *Polymer* **1989**, *30*, 1234.
- (14) Yoon, S. C.; Sung, Y. K.; Ratner, B. D. *Macromolecules* **1990**, *23*, 4351.
- (15) Kozlova, T. V.; Vdovina, S. V.; Zharkov, V. V. *Polym. Sci. USSR* **1991**, *33*, 749.
- (16) Yuying, X.; Zhiping, Z.; Dening, W.; Shengkang, Y.; Junxian, L. *Polymer* **1992**, *33*, 1335.
- (17) Seymour, R. W.; Estes, G. M.; Cooper, S. L. *Macromolecules* **1970**, *3*, 579.
- (18) Sung, C. S. P.; Schneider, N. S. *Macromolecules* **1975**, *8*, 68.
- (19) Eisenbach, C. D.; Gronski, W. *Makromol. Chem., Rapid Commun.* **1983**, *4*, 707.
- (20) Koberstein, J. T.; Gancarz, I.; Clarke, T. C. *J. Polym. Sci., Part B: Polym. Phys.* **1986**, *24*, 2487.
- (21) Lee, H. S.; Wang, Y. K.; Hsu, S. L. *Macromolecules* **1987**, *20*, 2089.
- (22) Lee, H. S.; Hsu, S. L. *Macromolecules* **1989**, *22*, 1100.
- (23) Estes, G. M.; Seymour, R. W.; Cooper, S. L. *Macromolecules* **1971**, *4*, 452.
- (24) Siesler, H. W. *Polym. Bull.* **1983**, *9*, 471.
- (25) Seymour, R. W.; Cooper, S. L. *Macromolecules* **1973**, *6*, 48.
- (26) MacKnight, W. J.; Yang, M. *J. Polym. Sci., Polym. Symp.* **1973**, *42*, 817.
- (27) Sung, C. S. P.; Schneider, N. S. *Macromolecules* **1977**, *10*, 452.
- (28) Senich, G. A.; MacKnight, W. J. *Macromolecules* **1980**, *13*, 106.
- (29) Dietrich, D.; Keberle, W.; Witt, H. *Angew. Chem., Int. Ed. Engl.* **1970**, *9*, 40.
- (30) Khranovskii, V. A.; Lipatov, Y. S.; Maslyuk, A. F. *Dokl. Phys. Chem.* **1985**, *285*, 1135.
- (31) Lipatov, Y. S.; Shilov, V. V.; Oleinik, S. P.; Bogdanovich, V. A.; Shelkovnikova, L. A. *Polym. Sci. USSR* **1986**, *28*, 2494.
- (32) Chan, W. C.; Chen, S. A. *Angew. Makromol. Chem.* **1988**, *163*, 77.
- (33) Chan, W. C.; Chen, S. A. *Polymer* **1988**, *29*, 1995.
- (34) Chen, S. A.; Chan, W. C. *J. Polym. Sci., Part B: Polym. Phys.* **1990**, *28*, 1499.
- (35) Chen, S. A.; Chan, W. C. *J. Polym. Sci., Part B: Polym. Phys.* **1990**, *28*, 1515.
- (36) Koenig, J. L. *Spectroscopy of Polymers*; American Chemical Society: Washington, DC, 1992.
- (37) Goddard, R. J.; Grady, B. P.; Cooper, S. L. *Macromolecules* **1994**, *27*, 1710.
- (38) Coleman, M. M.; Lee, K. H.; Skrovanek, D. J.; Painter, P. C. *Macromolecules* **1986**, *19*, 2149.
- (39) Bufalini, J.; Stern, K. H. *J. Am. Chem. Soc.* **1961**, *83*, 4362.
- (40) Allerhand, A.; Schleyer, P. V. R. *J. Am. Chem. Soc.* **1963**, *85*, 1233.
- (41) Goddard, R. J.; Cooper, S. L. *Macromolecules* **1995**, *28*, 1401.
- (42) Tsubomura, H. *J. Chem. Phys.* **1956**, *24*, 927.
- (43) Skrovanek, D. J.; Howe, S. E.; Painter, P. C.; Coleman, M. M. *Macromolecules* **1985**, *18*, 1676.
- (44) Skrovanek, D. J.; Painter, P. C.; Coleman, M. M. *Macromolecules* **1986**, *19*, 699.
- (45) Coleman, M. M.; Skrovanek, D. J.; Painter, P. C. *Makromol. Chem., Macromol. Symp.* **1986**, *5*, 21.
- (46) Boyarchuk, Y. M.; Rappoport, L. Y.; Nikitin, V. N.; Apukhtina, N. P. *Polym. Sci. USSR* **1965**, *7*, 859.
- (47) Hsu, S. L. *Acta Polym. Sin.* **1989**, *3*, 322.
- (48) Zharkov, V. V.; Strikovskiy, A. G.; Verteletskaya, T. E. *Polymer* **1993**, *34*, 938.
- (49) Wang, F. C.; Feve, M.; Lam, T. M.; Pascault, J. P. *J. Polym. Sci., Part B: Polym. Phys.* **1994**, *32*, 1315.
- (50) Wang, F. C.; Feve, M.; Lam, T. M.; Pascault, J. P. *J. Polym. Sci., Part B: Polym. Phys.* **1994**, *32*, 1305.

MA9413047